

# Fate of Majorana zero modes by a modified real-space-Pfaffian method and mobility edges in a one-dimensional quasiperiodic lattice

Shujie Cheng,<sup>1</sup> Yufei Zhu,<sup>2</sup> Gao Xianlong,<sup>1,\*</sup> and Tong Liu<sup>3,†</sup>

<sup>1</sup>*Department of Physics, Zhejiang Normal University, Jinhua 321004, China*

<sup>2</sup>*Department of Physics, University of Otago, P.O. Box 56, Dunedin 9054, New Zealand*

<sup>3</sup>*Department of Applied Physics, School of Science,*

*Nanjing University of Posts and Telecommunications, Nanjing 210003, China*

(Dated: July 20, 2021)

We aim to study a one-dimensional  $p$ -wave superconductor with quasiperiodic on-site potentials. A modified real-space-Pfaffian method is applied to calculate the topological invariants. We confirm that the Majorana zero mode is protected by the nontrivial topology the topological phase transition is accompanied by the energy gap closing and reopening. In addition, we numerically find that there are mobility edges which originate from the competition between the extended  $p$ -wave pairing and the localized quasi-disorder. We qualitatively analyze the influence of superconducting pairing parameters and on-site potential strength on the mobility edge. In general, our work enriches the research on the  $p$ -wave superconducting models with quasiperiodic potentials.

## I. INTRODUCTION

The Majorana fermion is a kind of particular particle, whose antiparticle is itself [1–3]. During the decade, the signatures of its presence have been found in many condensed matter systems, such as the semiconductor nanowires with strong spin-orbital couplings [4–8], ultracold atoms [9–12], magnetic atom chains [13–16], and the heterojunctions of normal superconductor and topological insulator [17–24]. Because of its application prospect in topological quantum computation [25, 26], the Majorana fermion has attracted extensive research interests [27–31].

The Majorana fermion is theoretically proven to exist in topological superconductors with  $p$ -wave pairings, which appears in Majorana zero mode (MZM) and are located at both ends of the system, and are protected by the topology [32]. As we all know, disorder will give rise to the localization phenomenon [33] which will result in the destruction of the topological non-trivial phases in topological superconductors [34–41]. Cai et al. [42] discussed the influence of the correlated disorder namely the quasiperiodic disorder on the MZM. They found that with the increase of the disorder potential, the system would undergo the transition from the topological non-trivial phase to the Anderson localized phase, that is, the MZM keeps robustness only to the weak disorder. Moreover, such a transition can be characterized by the quench dynamics [43] and the Kibble-Zurek mechanism [44]. Wang et al. [45] detailedly investigated the delocalization properties of the topological phase where the MZM exists, and revealed that it consists of an extended phase and a critical phase. Non-Hermiticity usually brings some novel phenomena, such as the anomalous boundary states [46] and the skin effect [47–49]. Re-

cent studies have shown that the MZM can appear in non-Hermitian  $p$ -wave superconductors [50, 51], and an unconventional real-complex transition of the energies is investigated [51].

From Kitaev’s seminal work, we know that the presence and absence of the above mentioned MZM can be characterized by the Pfaffian [32]. In principle, topological phase diagram of a generalized  $p$ -wave superconducting model can be further extracted by the Pfaffian method. However, due to the fact that this method is limited in those superconducting models possessing either homogeneous potential [32] or integer-periodic potential [52]. For the quasiperiodic  $p$ -wave superconducting models, the original Pfaffian method is no longer convenient in calculation. Therefore, in this paper, we will study the topological phase diagram of a  $p$ -wave superconducting model with a generalized potential by introducing a modified real-space-Pfaffian method. Besides, we will validate the efficiency of this method by other generations of Kitaev model. In addition, we note a fact that the Kitaev model with a homogeneous potential has the topological boundary located at  $V = 2t$  [32] while the quasiperiodic potential possesses a wider topological boundary [42, 45]. It is unpredictable that how the topological boundary changes when the homogeneous potential and the quasiperiodic potential coexist. Meanwhile, previous researches reveal that the homogeneous potential makes wave functions extended while the quasi-periodicity brings about the Anderson localization [42, 45, 53]. It is unknown whether there exists mobility edges when both two types of potentials coexist. In this paper, we will consider a special case that the potential consists of a homogeneous part and a quasiperiodic one, and make attempt to reveal the topological properties and mobility edges that this potential leads to.

The rest of this paper are organized as follows. In Sec. II, we introduce the Hamiltonian of a  $p$ -wave superconducting model with a general potential. In Sec. III, we first introduce the modified real-space-Pfaffian method,

\* gaoxl@zjnu.edu.cn

† t6tong@njupt.edu.cn

and then we discuss the topological properties and the mobility edges of the system. We make a brief summary in Sec. IV.

## II. MODEL AND HAMILTONIAN

Real quantum systems are more or less affected by disorder. In this paper, we study a one-dimensional  $p$ -wave superconductor with quasiperiodic disordered on-site potentials, which is described by the following tight-binding Hamiltonian

$$\hat{H} = \sum_{n=1}^{L-1} \left( -t\hat{c}_n^\dagger \hat{c}_{n+1} + \Delta\hat{c}_{n+1}^\dagger \hat{c}_n^\dagger + h.c. \right) + \sum_{n=1}^L V_n \hat{c}_n^\dagger \hat{c}_n \quad (1)$$

where  $\hat{c}_n$  ( $\hat{c}_n^\dagger$ ) denotes the fermion annihilation (creation) operator, and  $L$  is the size of the system with  $n$  being the site index. The nearest neighbor tunneling strength  $t$  and the nearest superconducting pairing parameter  $\Delta$  are real constants.  $t = 1$  is set as the unit of energy. The quasiperiodic on-site potential  $V_n$  is

$$V_n = \frac{V}{1 - b \cos(2\pi\alpha n)}, \quad (2)$$

where  $V$  is the potential strength,  $b \in (0, 1)$  is the modulation parameter, and  $\alpha = (\sqrt{5}-1)/2$  is the incommensurate modulation frequency. When  $b = 0$ , the model goes back to the Kitaev model [32], where  $V = 2t$  is the phase transition point, namely the topological boundary of the topological non-trivial phase ( $V < 2t$ ) and the topological trivial one ( $V > 2t$ ). The potential can be understood as the superposition of a homogeneous potential and incommensurate potentials with different frequencies

$$\begin{aligned} V_n &= \frac{V}{\tanh \beta} \cdot \frac{\sinh \beta}{\cosh \beta - \cos(2\pi\alpha n)} \\ &= \frac{V}{\tanh \beta} \sum_{r=-\infty}^{\infty} e^{-\beta|r|} e^{ir(2\pi\alpha n)} \\ &= \frac{V}{\tanh \beta} \left[ 1 + 2 \sum_{r=1}^{\infty} e^{-\beta r} \cos[r(2\pi\alpha n)] \right], \end{aligned} \quad (3)$$

where  $\cosh \beta = 1/b$  is the constraint condition. The parameter  $b$  controls the number of the summation terms. When  $b$  is small,  $V_n$  can be truncated into the summation with finite terms. As discussed before, the homogeneous potential manifests the topological boundary of  $p$ -wave superconductor located at  $V = 2t$ , whereas Cai et al. [42] and Wang et al. [45] show that the considered quasiperiodicity broadens the topological boundary. For our model, it is unknown how the fate of topological boundary changes when both two types of potentials coexist. In addition, we know that the homogeneous potentials keep the wave functions extended while the incommensurate potentials lead to the Anderson localization [42, 45, 53]. Whether there exist mobility edges is still unknown when

both two types of potentials coexist. In the next section, we will investigate these two aspects.

In the particle-hole picture, the Hamiltonian is diagonalized. In order to obtain the full energy spectrum, we shall introduce the Bogoliubov-de Gennes (BdG) transformation

$$\hat{\xi}_j^\dagger = \sum_{n=1}^L [u_{j,n} \hat{c}_n^\dagger + v_{j,n} \hat{c}_n], \quad (4)$$

where  $j$  ranges from 1 to  $L$  and the components  $u_{j,n}$  and  $v_{j,n}$  are real numbers. Thus, the Hamiltonian in Eq. (1) is diagonalized as

$$\hat{H} = \sum_{j=1}^L E_j (\hat{\xi}_j^\dagger \hat{\xi}_j - \frac{1}{2}), \quad (5)$$

where  $E_j$  is the eigenenergy which can be determined by the following BdG equations

$$\begin{cases} -t(u_{n-1} + u_{n+1}) + \Delta(v_{n-1} - v_{n+1}) + V_n u_n = E_j u_n, \\ t(v_{n-1} + v_{n+1}) + \Delta(u_{n+1} - u_{n-1}) - V_n v_n = E_j v_n. \end{cases} \quad (6)$$

Furthermore, we represent the wave function as the following form

$$|\psi_j\rangle = (u_{j,1}, v_{j,1}, u_{j,2}, v_{j,2}, \dots, u_{j,L}, v_{j,L})^T, \quad (7)$$

then, according to the BdG equations, we have the following BdG matrix

$$\mathcal{H} = \begin{pmatrix} A_1 & B & 0 & \cdots & \cdots & \cdots & C \\ B^\dagger & A_2 & B & 0 & \cdots & \cdots & 0 \\ 0 & B^\dagger & A_3 & B & 0 & \cdots & 0 \\ \vdots & \ddots & \ddots & \ddots & \ddots & \ddots & \vdots \\ 0 & \cdots & 0 & B^\dagger & A_{L-2} & B & 0 \\ 0 & \cdots & \cdots & 0 & B^\dagger & A_{L-1} & B \\ C^\dagger & \cdots & \cdots & \cdots & 0 & B^\dagger & A_L \end{pmatrix}, \quad (8)$$

where  $A_j = \begin{pmatrix} V_j & 0 \\ 0 & -V_j \end{pmatrix}$  and  $B = \begin{pmatrix} -t & -\Delta \\ \Delta & t \end{pmatrix}$ ;  $C$  is a null matrix when considering open boundary condition (OBC) and  $C = \begin{pmatrix} -t & \Delta \\ -\Delta & t \end{pmatrix}$  for the periodic boundary condition [45]. Intuitively,  $\mathcal{H}$  is a  $2L \times 2L$  matrix. By using the Schmidt orthogonal decomposition method to diagonalize the BdG matrix, we can acquire the full energy spectrum  $E_j$  and the associated wave functions  $|\psi_j\rangle$  directly. These strategies are favorable for studying the topological properties, such as the MZM and energy gap, as well as the mobility edges. These investigations will be presented in the following section.

## III. RESULTS AND DISCUSSIONS

The topological property of the system is directly characterized by a topological invariant. According to Kitaev's work, the Hamiltonian in Eq. (1) can be expanded

in terms of Majorana operators as

$$\hat{H} = \frac{i}{4} \sum_{\ell, m}^{2L} h_{\ell m} \lambda_{\ell} \lambda_m, \quad (9)$$

where  $h_{\ell m}$  is real antisymmetric matrix, satisfying

$$h_{\ell m}^* = h_{\ell m} = -h_{m\ell}, \quad (10)$$

and  $\lambda_{\ell}$  is the Majorana operator with  $\{\lambda_{\ell}, \lambda_m\} = 2\delta_{\ell m}$ , which is defined as

$$\begin{aligned} \lambda_{2n-1} &\equiv \hat{c}_{2n-1}^{\dagger} + \hat{c}_{2n-1} = \lambda_n^A, \\ \lambda_{2n} &\equiv i(\hat{c}_{2n}^{\dagger} - \hat{c}_{2n}) = \lambda_n^B. \end{aligned} \quad (11)$$

Accordingly, under PBC, the represented Hamiltonian is

$$\begin{aligned} \hat{H} = \frac{i}{4} &\left[ \sum_{n=1}^{L-1} (\Delta - t) \lambda_n^A \lambda_{n+1}^B + (\Delta + t) \lambda_n^B \lambda_{n+1}^A \right. \\ &+ \left. \sum_{n=1}^L V_n \lambda_n^A \lambda_n^B + (\Delta - t) \lambda_L^A \lambda_1^B - (t + \Delta) \lambda_1^A \lambda_L^B - h.c. \right]. \end{aligned} \quad (12)$$

For an antisymmetric matrix, its Pfaffian is defined as

$$\text{Pf}(h) = \frac{1}{2^{L} L!} \sum_{\tau \in S_{2L}} \text{sgn}(\tau) h_{\tau(1), \tau(2)} \cdots h_{\tau(2L-1), \tau(2L)}, \quad (13)$$

where  $S_{2L}$  denotes a series of permutations on these  $2L$  elements with  $\text{sgn}(\tau)$  being the sign of permutation. With the Pfaffian of the system, then the topological invariant  $M$  can be defined as [32, 42]

$$M = \text{sgn}(\text{Pf}(h)). \quad (14)$$

Although we known that we can calculate the Pfaffian to obtain the topological invariant of the  $p$ -wave superconducting system, Eq. (13) is appropriate for some special  $p$ -wave superconducting systems, such as the systems either with homogeneous potential [32] or with integer-periodic potential [52]. But for the quasiperiodic case, it is difficult to deal with the perturbation group operation directly. Therefore, we propose a modified real-space-Pfaffian method to conveniently calculate the topological invariant. This method require us to make a Schur decomposition [54] on the real anti-symmetric matrix  $h$

$$h = U D U^T, \quad (15)$$

where  $U$  is a unitary matrix, and  $D$  is an anti-symmetric tridiagonal matrix. Thus, the Pfaffian of  $h$  is redefined as

$$\text{Pf}(h) = \text{Det}(U) \text{Pf}(D), \quad (16)$$

$\text{Det}(U)$  is the determinant of the unitary matrix  $U$ . In practice, we can use Eqs. (14) and (16) to obtain the topological phase diagram, for the reason that  $\text{Det}(U)$

and  $\text{Pf}(D)$  are numerically available (see details in the Appendix).

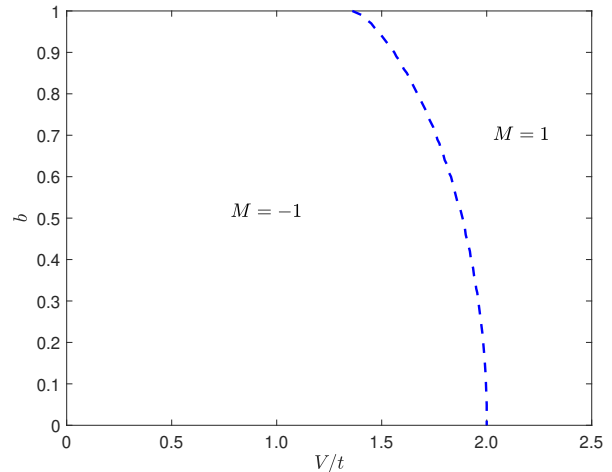


Figure 1. (Color Online)  $b$ - $V/t$  topological phase diagram for systems with  $\alpha = (\sqrt{5}-1)/2$ ,  $\Delta = 0.5t$ .  $M = -1$  corresponds to the topological non-trivial phase, and  $M = 1$  corresponds to the topological trivial phase. The blue dashed line denotes the phase boundary.

We calculate the Pfaffian by the proposed modified real-space-Pfaffian method, and naturally obtain the topological phase diagram of the system, which is presented in Fig. 1. The diagram shows that  $M = -1$  corresponds to the topological non-trivial phase, whereas  $M = 1$  corresponds to the topological trivial phase and the blue dashed line denotes the numerically obtained phase boundary. We know that when  $b = 0$ , our model goes back to the Kitaev model, whose transition is located at  $V = 2t$  [32]. We notice that when  $b$  is taken at small value, the phase transition is almost the same with that of the Kitaev model. This implies that our model is robust against the disordered perturbations. When  $b$  increases, the phase boundary bends in the direction of the decreasing  $V$ . This phenomenon is the direct result of the enhanced disorder effect, which compress the topological non-trivial region. It is to say that we can not only realize the topological phase transition by adjusting the potential strength  $V$ , but also manipulate the phase transition by controlling the strength of the disorder which is determined by the parameter  $b$  in our system.

In topological systems, the topological phase transition is accompanied with the gap closing and reopening. Figure 2 plots the energy gap  $\Delta_g$  as a function of the potential strength  $V$  with various  $b$ . The  $\Delta_g$  is defined as the difference of the  $(L+1)$ -th energy level and the  $L$ -th energy level under periodic boundary condition, i.e.  $\Delta_g = E_{L+1} - E_L$ . It is readily seen that when the topological phase transition happens, the gap undergoes closing and reopening. Different from the quasiperiodic case [42, 45], there appears a wider gap when system in the topological trivial phase. This phenomenon occurs

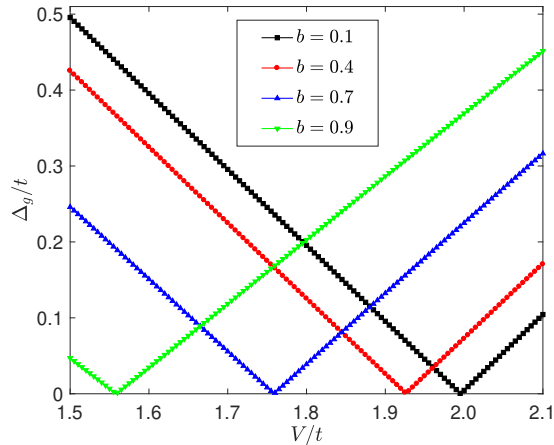


Figure 2. (Color Online) The energy gap  $\Delta_g$  versus  $V$  with various  $b$ . Other involved parameters are  $\alpha = (\sqrt{5} - 1)/2$ ,  $\Delta = 0.5t$ , and  $L = 1000$ .

because the uniform potential energy has more impact on the energy gap than that of quasi-periodic disordered perturbations [32, 42]. Moreover, when  $b$  is small, the gap closing point is almost at  $V = 2t$ . As  $b$  increases, the gap closing point moves towards the direction of the decreasing  $V$ . This feature is in accord with the topological boundary in Fig. 1.

The topological non-trivial phase implies the presence of the MZMs. Figure 3(a) shows the excitation energy spectrum as a function of the potential strength  $V$  under the open boundary condition. The spectrum reflects that the MZMs are only located in the topological non-trivial phase. To see the distributions of zero energy states, we rewrite the BdG operators as

$$\eta_j^\dagger = \frac{1}{2} \sum_{n=1}^L [\Phi_{j,n} \lambda_n^A - i \Psi_{j,n} \lambda_n^B], \quad (17)$$

where  $\Phi_{j,n} = (u_{j,n} + v_{j,n})$  and  $\Psi_{j,n} = (u_{j,n} - v_{j,n})$ .

Figures 3(b) and 3(c) respectively plot the spatial distributions  $\Phi$  and  $\Psi$  for the lowest excitation state with  $V = 1.5$ . Figures 3(d) and 3(e) are distributions for the lowest excitation state with  $V = 2t$ . When  $V = 1.5t$ , we know that the system is in the topological non-trivial phase, so the lowest excitation state is the Majorana zero energy state. As the figures show, the distributions of corresponding  $\Phi$  and  $\Psi$  are located at ends of the system, reflecting the bulk-boundary correspondence. The contrary consequence is that when  $V = 2t$ , the system is in the topological trivial phase and the corresponding  $\Phi$  and  $\Psi$  distribute in the bulk of the system. It is interpreted that the system is in the topological trivial phase and the lowest excitation state is no longer the Majorana edge state but the bulk state.

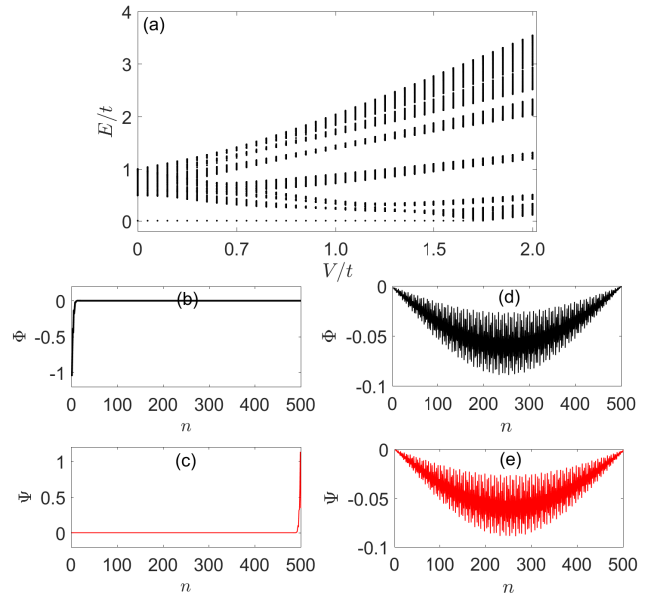


Figure 3. (Color Online) (a) Excitation energy spectrum of the system under the open boundary condition. (b) and (c) ((d) and (e)) are respectively the spatial distributions of  $\Phi$  and  $\Psi$  for the lowest excitation state with  $V = 1.5t$  ( $V = 2t$ ). Other involved parameters are  $L = 500$ ,  $b = 0.7$ ,  $\alpha = (\sqrt{5} - 1)/2$ , and  $\Delta = 0.5t$ .

We note that in the topological trivial phase, the spatial distributions of  $\Phi$  and  $\Psi$  for the lowest excitation state are no longer localized in the bulk but expand throughout the whole system, presenting an extended state. We are aware that such a phenomenon in this quasiperiodic superconducting system has relevance with the mobility edge instead of the Anderson localization [42, 45]. The localization-delocalization property can be characterized by the inverse participation ratio (IPR). For a given normalized wave function, the associated IPR is defined as

$$\text{IPR}_j = \sum_{n=1}^L (|u_{j,n}|^4 + |v_{j,n}|^4). \quad (18)$$

It is well known that for an extended wave function, the IPR scales like  $L^{-1}$  and it approaches 1 for a localized wave function. We consider  $b = 0.7$  as an example to verify the above surmise and make an attempt to qualitatively analyze the influence of the superconducting pairing parameter  $\Delta$  on the mobility edge. By taking four different  $\Delta$ , we plot the excitation spectra and IPR as a function of  $V$  under PBC, which are shown in Fig. 4(a), 4(b), 4(c), and 4(d) respectively. According to the numerical results, the distinction between the extended states and the localized states can be readily seen from the IPR (the color bar shows). The transition boundary in energy is just the mobility edge. When  $\Delta$  is small, the low-energy excitation states are extended states, while those states with higher energy are localized. When  $\Delta$  gets larger, the mobility edge moves towards the

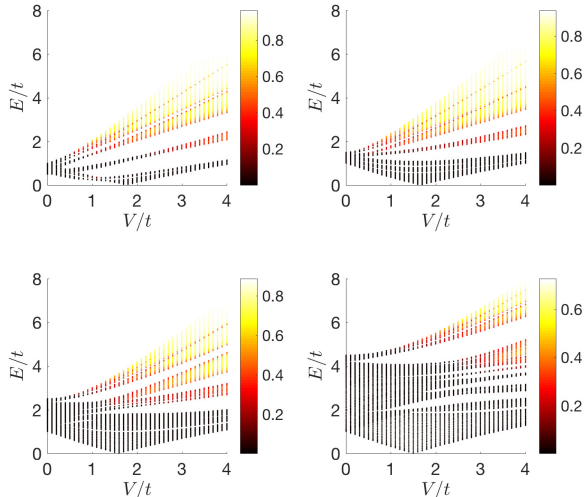


Figure 4. (Color Online) The excitation spectrum and IPR as a function of  $V$  with  $\Delta = 0.5t$  in (a),  $\Delta = 1.5t$  in (b),  $\Delta = 2.5t$  in (c), and  $\Delta = 4.5t$  in (d). Other involved parameters are  $b = 0.7$ ,  $\alpha = (\sqrt{5} - 1)/2$ , and  $L = 500$ .

high-energy region. Moreover, we notice that when the quasiperiodic potential strength  $V$  is small, all the excitation states are extended. Moreover, the extended region gets larger when  $\Delta$  increases. In other words, the superconducting pairing is robust against the weak disorder and makes the system more extended. From Fig. 4(a), we also notice that when  $V = 2t$ , the IPR of the lowest excitation state approaches zero, signaling the extended state. The result answers why the  $\Psi$  and  $\Psi$  in Fig. 3(d) and 3(e) distribute throughout the whole system.

#### IV. SUMMARY

Herin, a quasiperiodic  $p$ -wave superconducting model with coexistence of the homogeneous potential and

quasiperiodic potential has been investigated. We proposed a modified real-space-Pfaffian method, which is beneficial and accurate to obtain the topological invariant of this system. We have demonstrated that the topological phases are protected by the gap. However, compared to the purely quasiperiodic case, the gap in the topological nontrivial is more wider. We have argued that this phenomenon occurs because the homogeneous potential has more impact on the gap. Besides, we have uncovered that there are mobility edges in the  $p$ -wave superconducting model. We have argued that the mobility edge originates from the competition between the extended  $p$ -wave pairing and the localized quasi-disorder. Furthermore, we have discussed the influence of the superconducting pairing parameter on the mobility edge. From the analysis, we have arrived at a qualitative fact that superconducting pairings tend to make system extended and stronger pairings move the mobility edge towards to high-energy region. In general, our theoretical work, i.e., the modified real-space Pfaffian method, overcomes the technical problem of using Pfaffian method to solve the topological invariants of a general  $p$ -wave superconductor and makes up for the limitation of the original Pfaffian. Moreover, the uncovered mobility edges promote a further understanding on the quasiperiodic  $p$ -wave superconductors. We note that a similar potential has been realized by the Raman coupling [55] and the  $p$ -wave pairings can be induced by the superconducting proximity effect [3]. We expect that these intriguing quantum phenomena predicted in our study will be realized in near future experiments by means of these experimental techniques.

#### V. ACKNOWLEDGE

Gao Xianlong and Shujie Cheng acknowledge the support from NSFC under Grants No.11835011 and No.11774316. Tong Liu acknowledges Natural Science Foundation of Jiangsu Province (Grant No. BK20200737) and NUPTSF (Grant No.NY220090 and No.NY220208).

#### Appendix: Modified real-space-Pfaffian method

As mentioned in the main text, we can perform a Schur decomposition [54] on a general anti-symmetric matrix  $h$ , i.e.,  $h = UDU^T$ . After this operation, we obtain a  $2L \times 2L$  anti-symmetric tridiagonal matrix  $D$ , which has the following configuration

$$D = \begin{pmatrix} 0 & a_1 & & & & & \\ -a_1 & 0 & b_1 & & & & \\ & -b_1 & 0 & a_2 & & & O \\ & & -a_2 & \ddots & \ddots & & \\ & & & \ddots & 0 & b_{L-1} & \\ O & & & & -b_{L-1} & 0 & a_L \\ & & & & & -a_L & 0 \end{pmatrix}. \quad (\text{A.1})$$

According to the original definition of the Pfaffian (Eq. (13)), we can easily obtain the Pfaffian of the matrix  $D$ , which is given as

$$\text{Pf}(D) = \prod_{i=1}^L a_i. \quad (\text{A.2})$$

Therefore, to obtain the Pfaffian of a general anti-symmetric matrix  $h$ , a standard strategy is that we first calculate to unitary matrix  $U$  and the target matrix  $D$  by the Schur decomposition, and then obtain the Pfaffian of  $D$  by Eq. (A.2), and finally obtain the Pfaffian of  $h$  by Eq. (16). We name the Pfaffian method after Schur decomposition as the modified real-space-Pfaffian method. In the following, we will show that how this method is effectively applied to obtain the topological phase diagram of  $p$ -wave superconducting models.

- 1) Test on the Kitaev model [32] ( $V_n = V$ ). We consider  $t = 1$ ,  $\alpha = (\sqrt{5} - 1)/2$ ,  $\Delta = 0.5t$  and  $L = 5$  in all our tests.  $V = 1.5t$  and  $V = 2.5t$  are two chosen parameters. We have known that the topological boundary is located at  $V_c = 2t$ . Therefore,  $V = 1.5t$  corresponds to the topological non-trivial phase, and gives  $M = -1$ ;  $V = 2.5t$  corresponds to the topological non-trivial phase, and gives  $M = 1$ ; Taking  $V = 1.5t$  and other parameters into  $h$ , and performing the Schur decomposition, we have

$$U = \begin{pmatrix} 0 & -0.44721 & 0.62997 & -0.019914 & 0.052389 & 0 & -0.18026 & 0 & 0.60622 & 0 \\ 0.44721 & 0 & -0.019876 & -0.62876 & 0 & 0.065277 & 0 & 0.32194 & 0 & 0.54439 \\ 0 & -0.44721 & -0.54043 & 0.017083 & 0.32809 & 0 & -0.63226 & 0 & 0.015899 & 0 \\ 0.4721 & 0 & 0.014868 & 0.47033 & 0 & -0.42257 & 0 & -0.41826 & 0 & 0.47441 \\ 0 & -0.44721 & 0.24447 & -0.0077279 & -0.58324 & 0 & -0.21050 & 0 & -0.59640 & 0 \\ 0.44721 & 0 & -0.0041805 & -0.13225 & 0 & 0.61846 & 0 & -0.58043 & 0 & -0.25119 \\ 0 & -0.44721 & 0.14487 & -0.0045795 & 0.61562 & 0 & 0.50216 & 0 & -0.38449 & 0 \\ 0.44721 & 0 & -0.0081034 & -0.25635 & 0 & -0.57812 & 0 & 0.059529 & 0 & -0.62965 \\ 0 & -0.44721 & -0.47888 & 0.015138 & -0.41285 & 0 & 0.52085 & 0 & 0.35877 & 0 \\ 0.44721 & 0 & 0.017292 & 0.54703 & 0 & 0.31695 & 0 & 0.61723 & 0 & -0.13796 \end{pmatrix}, \quad (\text{A.3})$$

and

$$D = \begin{pmatrix} 0 & -0.50 & 0 & 0 & 0 & 0 & 0 & 0 & 0 & 0 \\ 0.50 & 0 & 0 & 0 & 0 & 0 & 0 & 0 & 0 & 0 \\ 0 & 0 & 0 & -3.1730 & 0 & 0 & 0 & 0 & 0 & 0 \\ 0 & 0 & 3.1730 & 0 & 0 & 0 & 0 & 0 & 0 & 0 \\ 0 & 0 & 0 & 0 & 0 & -3.1730 & 0 & 0 & 0 & 0 \\ 0 & 0 & 0 & 0 & 3.1730 & 0 & 0 & 0 & 0 & 0 \\ 0 & 0 & 0 & 0 & 0 & 0 & 0 & 1.2971 & 0 & 0 \\ 0 & 0 & 0 & 0 & 0 & 0 & -1.2971 & 0 & 0 & 0 \\ 0 & 0 & 0 & 0 & 0 & 0 & 0 & 0 & 0 & 1.2971 \\ 0 & 0 & 0 & 0 & 0 & 0 & 0 & 0 & -1.2971 & 0 \end{pmatrix}. \quad (\text{A.4})$$

It is easy to get  $\text{Det}(U) = 1$  and  $\text{Pf}(D) = -8.4688$ . According to Eq. (16), we obtain the topological invariant  $M = \text{sgn}(\text{Pf}(h)) = -1$ . Next, we take  $V = 2.5t$  and other parameters into  $h$ . After performing the Schur decomposition, we have

$$U = \begin{pmatrix} -0.41412 & -0.16884 & -0.0048475 & 0.63189 & -0.026194 & 0.0015328 & -0.0071719 & 0.62251 & 0.11151 & 0 \\ -0.16884 & 0.41412 & -0.62926 & -0.0048273 & -0.0036987 & -0.063207 & 0.5053 & 0.0058216 & 0 & 0.38031 \\ -0.41412 & -0.16884 & 0.00404 & -0.52663 & -0.3496 & 0.020458 & -0.0034379 & 0.29841 & -0.55762 & 0 \\ -0.16884 & 0.41412 & 0.47187 & 0.0036199 & 0.0246 & 0.42038 & 0.51782 & 0.0059658 & 0 & -0.36308 \\ -0.41412 & -0.16884 & -0.0016894 & 0.22022 & 0.59186 & -0.034635 & 0.0050471 & -0.43808 & -0.45614 & 0 \\ -0.16884 & 0.41412 & -0.13424 & -0.0010298 & -0.036105 & -0.61699 & -0.18527 & -0.0021345 & 0 & -0.60471 \\ -0.41412 & -0.16884 & -0.0013065 & 0.17031 & -0.60805 & 0.035582 & 0.0065572 & -0.56916 & 0.27571 & 0 \\ -0.16884 & 0.41412 & -0.25467 & -0.0019537 & 0.033819 & 0.57793 & -0.63232 & -0.007285 & 0 & -0.010648 \\ -0.41412 & -0.16884 & 0.0038034 & -0.49579 & 0.39199 & -0.022938 & -0.00099451 & 0.0086322 & 0.62654 & 0 \\ -0.16884 & 0.41412 & 0.5463 & 0.0041909 & -0.018615 & -0.31811 & -0.20553 & -0.0023678 & 0 & 0.59813 \end{pmatrix}, \quad (\text{A.5})$$

and

$$D = \begin{pmatrix} 0 & -0.50 & 0 & 0 & 0 & 0 & 0 & 0 & 0 & 0 \\ 0.50 & 0 & 0 & 0 & 0 & 0 & 0 & 0 & 0 & 0 \\ 0 & 0 & 0 & 4.1598 & 0 & 0 & 0 & 0 & 0 & 0 \\ 0 & 0 & -4.1598 & 0 & 0 & 0 & 0 & 0 & 0 & 0 \\ 0 & 0 & 0 & 0 & 0 & -4.1598 & 0 & 0 & 0 & 0 \\ 0 & 0 & 0 & 0 & 4.1598 & 0 & 0 & 0 & 0 & 0 \\ 0 & 0 & 0 & 0 & 0 & 0 & 0 & -2.1086 & 0 & 0 \\ 0 & 0 & 0 & 0 & 0 & 0 & 2.1086 & 0 & 0 & 0 \\ 0 & 0 & 0 & 0 & 0 & 0 & 0 & 0 & 0 & 2.1086 \\ 0 & 0 & 0 & 0 & 0 & 0 & 0 & 0 & -2.1086 & 0 \end{pmatrix}. \quad (\text{A.6})$$

In this case, we have  $\text{Det}(U) = -1$  and  $\text{Pf}(D) = -3.8469$ . According to Eq. (16), we get  $M = 1$ . If leaving the  $V$  changing while other parameters invariable, by means of this method, we can obtain the topological phase diagram of the Kitaev model, as shown in Fig. 5.

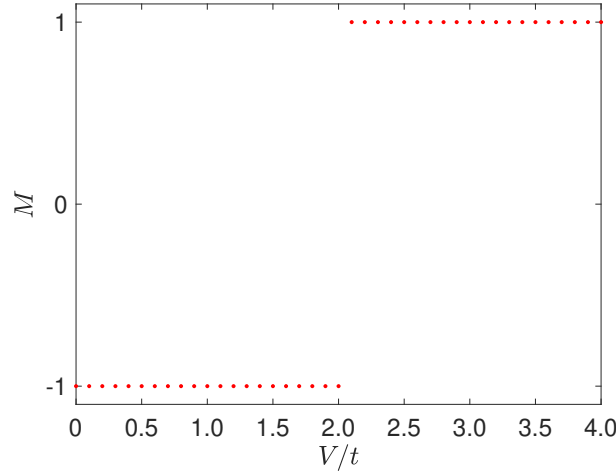


Figure 5. (Color Online)  $M - V/t$  topological phase diagram of the Kitaev model.

- 2) Test on the quasiperiodic  $p$ -wave superconducting model [42, 45]. This model requires  $V_n = V \cos(2\pi\alpha n)$ , and its topological boundary is located at  $V_c = 2t + 2\Delta$ . Without loss of generality, we take  $\Delta = 0.5t$ , thus the topological boundary is  $V_c = 3t$ .  $V = 2.8t$  and  $V = 3.2t$  are two chosen parameters, corresponding to the topological non-trivial phase ( $M = -1$ ) and topological trivial phase ( $M = 1$ ) respectively. We first test the case with  $V = 2.8t$ . After performing the Schur decomposition, we get

$$U = \begin{pmatrix} -0.10292 & -0.086979 & -0.014115 & -0.75278 & -0.048208 & -0.38713 & 0.077204 & 0.14370 & 0.48596 & -1.8239e-04 \\ -0.024698 & 0.029224 & 0.60102 & -0.011270 & -0.45909 & 0.057169 & -0.57104 & 0.30680 & 2.0348e-05 & 0.054217 \\ 0.057680 & 0.048749 & -6.3534e-03 & -0.33884 & -0.012153 & -0.097596 & 0.25378 & 0.47234 & -0.76306 & 2.8639e-04 \\ 0.041361 & -0.048939 & 0.027242 & -5.1081e-04 & -0.55188 & 0.068724 & 0.31347 & -0.16842 & -2.8067e-04 & -0.74782 \\ -0.071450 & -0.060387 & 2.6104e-03 & 0.13922 & -0.10006 & -0.80349 & -0.22492 & -0.41864 & -0.30068 & 1.1285e-04 \\ -0.24982 & 0.29559 & 0.31525 & -5.9112e-03 & 0.62080 & -0.077306 & -0.15776 & 0.084763 & -2.1473e-04 & -0.57214 \\ 0.59525 & 0.50308 & -7.1582e-03 & -0.38176 & 0.018809 & 0.15104 & -0.21896 & -0.40753 & -0.097991 & 3.6778e-05 \\ -0.54896 & 0.64954 & 0.12755 & -2.3916e-03 & -0.23261 & 0.028966 & 0.31620 & -0.16989 & 1.0393e-04 & 0.27691 \\ 0.45824 & 0.38728 & 7.3351e-03 & 0.39119 & -0.049331 & -0.39615 & 0.23475 & 0.43692 & 0.28560 & -1.0719e-04 \\ 0.22490 & -0.26611 & 0.72251 & -0.013548 & 0.17289 & -0.021530 & 0.47621 & -0.25586 & 6.9004e-05 & 0.18386 \end{pmatrix}, \quad (\text{A.7})$$

and

$$D = \begin{pmatrix} 0 & -3.5300 & 0 & 0 & 0 & 0 & 0 & 0 & 0 & 0 & 0 \\ 3.5300 & 0 & 0 & 0 & 0 & 0 & 0 & 0 & 0 & 0 & 0 \\ 0 & 0 & 0 & -3.1062 & 0 & 0 & 0 & 0 & 0 & 0 & 0 \\ 0 & 0 & 3.1062 & 0 & 0 & 0 & 0 & 0 & 0 & 0 & 0 \\ 0 & 0 & 0 & 0 & 0 & 2.4913 & 0 & 0 & 0 & 0 & 0 \\ 0 & 0 & 0 & 0 & -2.4913 & 0 & 0 & 0 & 0 & 0 & 0 \\ 0 & 0 & 0 & 0 & 0 & 0 & 0 & -2.1429 & 0 & 0 & 0 \\ 0 & 0 & 0 & 0 & 0 & 0 & 0 & 2.1429 & 0 & 0 & 0 \\ 0 & 0 & 0 & 0 & 0 & 0 & 0 & 0 & 0 & 0 & -0.028422 \\ 0 & 0 & 0 & 0 & 0 & 0 & 0 & 0 & 0 & 0.028422 & 0 \end{pmatrix}. \quad (\text{A.8})$$

In this case, we have  $\text{Det}(U) = -1$  and  $\text{Pf}(D) = 1.6637$ . Therefore, the topological invariant is  $M = \text{sgn}(\text{Det}(U)\text{Pf}(D)) = -1$ . Next, we take  $V = 3.2t$  and other parameters into  $h$ . After performing the Schur decomposition, we obtain

$$U = \begin{pmatrix} 0.011327 & -0.13876 & 0.10555 & 0.73415 & -0.42287 & -0.076369 & -0.14586 & -0.11929 & 0.45864 & 1.0053\text{e-}04 \\ 0.012075 & 9.8569\text{e-}04 & -0.58865 & 0.084633 & -0.094622 & 0.52394 & 0.37923 & -0.46370 & 1.3679\text{e-}05 & -0.062405 \\ -0.0045091 & 0.055237 & 0.043898 & 0.30532 & -0.12858 & -0.023222 & -0.37712 & -0.30842 & -0.80459 & -1.7636\text{e-}04 \\ -0.057731 & -0.0047127 & -0.020556 & 0.0029554 & -0.087289 & 0.48334 & -0.23696 & 0.28974 & -1.7188\text{e-}04 & 0.78414 \\ 0.0075514 & -0.092506 & -0.020357 & -0.14159 & -0.74798 & -0.13508 & 0.43505 & 0.35580 & -0.27810 & -6.0959\text{e-}05 \\ 0.35934 & 0.029334 & -0.30339 & 0.043620 & 0.11036 & -0.61106 & 0.18838 & -0.23034 & -1.2045\text{e-}04 & 0.54949 \\ -0.064434 & 0.78933 & 0.056941 & 0.39604 & 0.16551 & 0.029890 & 0.32728 & 0.26766 & -0.075370 & -1.6521\text{e-}05 \\ 0.85592 & 0.069870 & -0.16543 & 0.023785 & -0.033619 & 0.18615 & -0.23825 & 0.29132 & 5.2414\text{e-}05 & -0.23912 \\ -0.047563 & 0.58265 & -0.059396 & -0.41311 & -0.43149 & -0.077926 & -0.37328 & -0.30528 & 0.24346 & 5.3365\text{e-}05 \\ -0.35803 & -0.029226 & -0.71653 & 0.10302 & 0.041274 & -0.22854 & -0.32950 & 0.40290 & 3.2591\text{e-}05 & -0.14868 \end{pmatrix}, \quad (\text{A.9})$$

and

$$D = \begin{pmatrix} 0 & 3.8730 & 0 & 0 & 0 & 0 & 0 & 0 & 0 & 0 & 0 \\ -3.8730 & 0 & 0 & 0 & 0 & 0 & 0 & 0 & 0 & 0 & 0 \\ 0 & 0 & 0 & -3.3699 & 0 & 0 & 0 & 0 & 0 & 0 & 0 \\ 0 & 0 & 3.3699 & 0 & 0 & 0 & 0 & 0 & 0 & 0 & 0 \\ 0 & 0 & 0 & 0 & 0 & 2.6843 & 0 & 0 & 0 & 0 & 0 \\ 0 & 0 & 0 & 0 & -2.6843 & 0 & 0 & 0 & 0 & 0 & 0 \\ 0 & 0 & 0 & 0 & 0 & 0 & 0 & -2.3647 & 0 & 0 & 0 \\ 0 & 0 & 0 & 0 & 0 & 0 & 2.3647 & 0 & 0 & 0 & 0 \\ 0 & 0 & 0 & 0 & 0 & 0 & 0 & 0 & 0 & 0 & -0.047520 \\ 0 & 0 & 0 & 0 & 0 & 0 & 0 & 0 & 0 & 0.047520 & 0 \end{pmatrix}. \quad (\text{A.10})$$

Along the same strategy, we have  $\text{Det}(U) = -1$  and  $\text{Pf}(D) = -3.9369$ , so the topological invariant is  $M = \text{sgn}(\text{Det}(U)\text{Pf}(D)) = 1$ . If we change the  $V$  continuously and keep other parameters invariable, then we can obtain the topological phase diagram, as shown in Fig. 6.

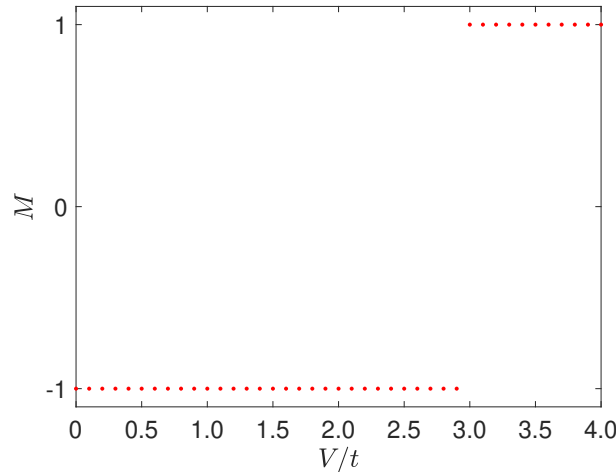


Figure 6. (Color Online)  $M - V/t$  topological phase diagram of the quasiperiodic  $p$ -wave superconducting model.



- 3) Test on our model (see Eq. (1)). The potential has been presented in Eq. (2). We consider  $b = 0.95$  in our test. According to the topological phase diagram in Fig. (1), we know the numerical topological boundary is located at about  $V_c = 1.5t$ .  $V = 1.2t$  and  $V = 1.7t$  are two chosen parameters, corresponding to the topological non-trivial phase and topological trivial phase respectively. We first test the case with  $V = 1.2t$ . After performing the Schur decomposition, we have

$$U = \begin{pmatrix} -0.023316 & -0.23546 & -0.094225 & 0.063506 & 0.31829 & 0.046668 & 0.85945 & 4.9924e-04 & -0.29822 & -5.4378e-03 \\ -0.10571 & 0.010468 & -0.092276 & -0.13691 & 0.11105 & -0.75736 & -1.6668e-04 & 0.28693 & -9.8719e-03 & 0.54139 \\ 2.4810e-03 & 0.025054 & 0.28855 & -0.19447 & -0.83687 & -0.12270 & 0.39619 & 2.3014e-04 & 0.076820 & 1.4008e-03 \\ 0.016300 & -1.6141e-03 & 0.26911 & 0.39929 & -0.069709 & 0.47543 & -2.0030e-04 & 0.34482 & -0.011788 & 0.64649 \\ 2.9746e-03 & 0.030039 & -0.71121 & 0.47934 & -0.24651 & -0.036144 & 0.13654 & 7.9316e-05 & 0.42745 & 7.7944e-03 \\ 0.035612 & -3.5265e-03 & -0.47172 & -0.69990 & -0.058984 & 0.40229 & -1.7914e-04 & 0.30839 & -2.9356e-03 & 0.16099 \\ -0.010398 & -0.10500 & 0.29848 & -0.20117 & 0.31062 & 0.045544 & 0.19598 & 1.1384e-04 & 0.84976 & 0.015495 \\ -0.23504 & 0.023275 & 0.090986 & 0.13500 & 8.1582e-03 & -0.055641 & -4.7133e-04 & 0.81139 & 9.2280e-03 & -0.50607 \\ 0.095100 & 0.96036 & 0.024252 & -0.016345 & 0.14154 & 0.020753 & 0.21754 & 1.2636e-04 & 4.4215e-03 & 8.0623e-05 \\ 0.96038 & -0.095103 & 0.025035 & 0.037146 & 0.017590 & -0.11997 & -1.2366e-04 & 0.21288 & 1.4808e-03 & -0.081207 \end{pmatrix}, \quad (\text{A.11})$$

and

$$D = \begin{pmatrix} 0 & -6.4697 & 0 & 0 & 0 & 0 & 0 & 0 & 0 & 0 \\ 6.4697 & 0 & 0 & 0 & 0 & 0 & 0 & 0 & 0 & 0 \\ 0 & 0 & 0 & 3.7355 & 0 & 0 & 0 & 0 & 0 & 0 \\ 0 & 0 & -3.7355 & 0 & 0 & 0 & 0 & 0 & 0 & 0 \\ 0 & 0 & 0 & 0 & 0 & -1.8606 & 0 & 0 & 0 & 0 \\ 0 & 0 & 0 & 0 & 1.8606 & 0 & 0 & 0 & 0 & 0 \\ 0 & 0 & 0 & 0 & 0 & 0 & 0 & -0.33654 & 0 & 0 \\ 0 & 0 & 0 & 0 & 0 & 0 & 0.33654 & 0 & 0 & 0 \\ 0 & 0 & 0 & 0 & 0 & 0 & 0 & 0 & 0 & -0.60564 \\ 0 & 0 & 0 & 0 & 0 & 0 & 0 & 0 & 0.60564 & 0 \end{pmatrix}. \quad (\text{A.12})$$

Easily, we have  $\text{Det}(U) = -1$  and  $\text{Pf}(D) = 9.1651$ . Therefore, the topological invariant is  $M = \text{sgn}(\text{Det}(U)\text{Pf}(D)) = -1$ . Next, we test the case with  $V = 1.7t$ . In the same way, we perform the Schur decomposition, then we get

$$U = \begin{pmatrix} -2.6224e-07 & 0.17518 & 0.056526 & -0.050351 & -0.37571 & -0.033873 & -0.52435 & 2.0649e-05 & 0.73915 & 9.0440e-04 \\ -0.077407 & -1.1588e-07 & -0.072657 & -0.081567 & 0.062177 & -0.68965 & -1.8448e-05 & -0.46847 & -6.5106e-04 & 0.53210 \\ 2.1014e-08 & -0.014037 & -0.21481 & 0.19135 & 0.85794 & 0.077350 & -0.090087 & 3.5476e-06 & 0.40852 & 4.9985e-04 \\ 0.0099040 & 1.4826e-08 & 0.27022 & 0.30336 & -0.055726 & 0.61809 & -1.6487e-05 & -0.41867 & -6.4098e-04 & 0.52385 \\ 2.5680e-08 & -0.017155 & 0.67495 & -0.60122 & 0.22258 & 0.020067 & 0.28462 & -1.1208e-05 & 0.22745 & 2.7831e-04 \\ 0.019830 & 2.9685e-08 & -0.59529 & -0.66829 & -0.031601 & 0.35050 & -1.6615e-07 & -0.0042191 & -3.3454e-04 & 0.27341 \\ -1.1364e-07 & 0.075912 & -0.22895 & 0.20394 & -0.23432 & -0.021126 & 0.79666 & -3.1372e-05 & 0.45848 & 5.6099e-04 \\ -0.17437 & -2.6104e-07 & 0.096535 & 0.10837 & 0.0063677 & -0.070628 & 3.0359e-05 & 0.77094 & -7.2301e-04 & 0.59089 \\ 1.4691e-06 & -0.98136 & -0.016346 & 0.014560 & -0.10135 & -0.0091379 & -0.035661 & 1.4043e-06 & 0.15759 & 1.9282e-04 \\ 0.98138 & 1.4691e-06 & 0.020723 & 0.023265 & 0.0072366 & -0.080266 & 4.1090e-06 & 0.10434 & -1.6659e-04 & 0.13615 \end{pmatrix}, \quad (\text{A.13})$$

and

$$D = \begin{pmatrix} 0 & 8.8733 & 0 & 0 & 0 & 0 & 0 & 0 & 0 & 0 \\ -8.8733 & 0 & 0 & 0 & 0 & 0 & 0 & 0 & 0 & 0 \\ 0 & 0 & 0 & -4.7433 & 0 & 0 & 0 & 0 & 0 & 0 \\ 0 & 0 & 4.7433 & 0 & 0 & 0 & 0 & 0 & 0 & 0 \\ 0 & 0 & 0 & 0 & 0 & 2.3372 & 0 & 0 & 0 & 0 \\ 0 & 0 & 0 & 0 & -2.3372 & 0 & 0 & 0 & 0 & 0 \\ 0 & 0 & 0 & 0 & 0 & 0 & 0 & 0.79243 & 0 & 0 \\ 0 & 0 & 0 & 0 & 0 & 0 & -0.79243 & 0 & 0 & 0 \\ 0 & 0 & 0 & 0 & 0 & 0 & 0 & 0 & 0 & 0.089008 \\ 0 & 0 & 0 & 0 & 0 & 0 & 0 & 0 & -0.089008 & 0 \end{pmatrix}. \quad (\text{A.14})$$

After calculation, we have  $\text{Det}(U) = -1$  and  $\text{Pf}(D) = -6.9383$ . Therefore, in this case, the topological invariant is  $M = \text{sgn}(\text{Det}(U)\text{Pf}(D)) = 1$ . If we change  $V$  continuously and leave other parameters invariable, then we can obtain the topological phase diagram, as shown in Fig. 7.

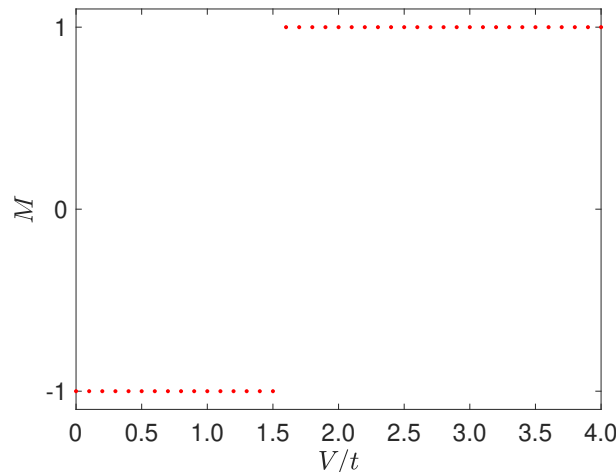


Figure 7. (Color Online)  $M - V/t$  topological phase diagram of our model.

From the above tests, it is readily seen that this modified real-space-Pfaffian method is very convenient and accurate to numerically obtain the topological phase diagram of  $p$ -wave superconducting model.

- 
- [1] X. L. Qi and S. C. Zhang, Topological insulators and superconductors, *Rev. Mod. Phys.* **83**, 1057 (2011).
- [2] S.-Q. Shen, *Topological Insulators* (Springer-Verlag, Berlin, 2012).
- [3] R. Aguado, Majorana quasiparticles in condensed matter, *Riv. Nuovo Cimento* **40**, 523 (2017).
- [4] V. Mourik, K. Zuo, S. M. Frolov, S. R. Plissard, E. P. A. M. Bakkers, and L. P. Kouwenhoven, Signatures of Majorana Fermions in Hybrid Superconductor-Semiconductor Nanowire Devices, *Science* **336**, 1003 (2012).
- [5] S. M. Albrecht, A. P. Higginbotham, M. Madsen, F. Kuemmeth, T. S. Jepserson, J. Nygard, P. Krogstrup, and C. M. Marcus, Exponential protection of zero modes in Majorana islands, *Nature* **531**, 206 (2016).
- [6] M. T. Deng, S. Vaitiekenas, E. B. Hansen, J. Danon, M. Leijnse, K. Flensberg, J. Nygard, P. Krogstrup, and C. M. Marcus, Majorana bound states in a coupled quantum-dot hybrid-nanowire system, *Science* **354**, 1557 (2016).
- [7] J. Chen, P. Yu, J. Stenger, M. Hocevar, D. Car, S. R. Plissard, E. P. A. M. Bakkers, T. D. Stanescu, and S. M. Frolov, Experimental phase diagram of zero-bias conductance peaks in superconductor/semiconductor nanowire devices, *Sci. Adv.* **3**, e1701476 (2017).
- [8] J. Klinovaja, P. Stano, and D. Loss, Transition from Fractional to Majorana Fermions in Rashba Nanowires, *Phys. Rev. Lett.* **109**, 236801 (2012).
- [9] X. J. Liu, L. Jiang, H. Pu, and H. Hu, Probing Majorana fermions in spin-orbit coupled atomic Fermi gases, *Phys. Rev. A* **85**, 021603(R) (2012).
- [10] C. Qu, Z. Zheng, M. Gong, Y. Xu, L. Mao, X. Zou, G. Guo, and C. Zhang, Topological superfluids with finite-momentum pairing and Majorana fermions, *Nat. Commun.* **4**, 2710 (2013).
- [11] C. Chen, Inhomogeneous Topological Superfluidity in One-Dimensional Spin-Orbit-Coupled Fermi Gases, *Phys. Rev. Lett.* **111**, 235302 (2013).
- [12] J. Ruhman, E. Berg, and E. Altman, Topological States in a One-Dimensional Fermi Gas with Attractive Interaction, *Phys. Rev. Lett.* **114**, 100401 (2015).
- [13] S. Nadj-Perge, I. K. Drozdov, B. A. Bernevig, and A. Yazdani, Proposal for realizing Majorana fermions in chains of magnetic atoms on a superconductor, *Phys. Rev. B* **88**, 020407(R) (2013).
- [14] S. Nadj-Perge, I. K. Drozdov, J. Li, H. Chen, S. Jeon, J. Seo, A. H. MacDonald, B. A. Bernevig, and A. Yazdani, Observation of Majorana fermions in ferromagnetic atomic chains on a superconductor, *Science* **346**, 602 (2014).
- [15] E. Dumitrescu, B. Roberts, S. Tewari, J. D. Sau, and S. D. Sarma, Majorana fermions in chiral topological ferromagnetic nanowires, *Phys. Rev. B* **91**, 094505 (2015).
- [16] S. Jeon, Y. L. Xie, Z. J. Wang, B. A. Bernevig, and A. Yazdani, Distinguishing a Majorana zero mode using spin-resolved measurements, *Science* **358**, 772 (2017).
- [17] L. Fu and C. L. Kane, Superconducting Proximity Effect and Majorana Fermions at the Surface of a Topological Insulator, *Phys. Rev. Lett.* **100**, 096407 (2008).
- [18] A. Cook and M. Franz, Majorana fermions in a topological-insulator nanowire proximity-coupled to an  $s$ -wave superconductor, *Phys. Rev. B* **84**, 201105 (2011).
- [19] Y. Tanaka, M. Sato, and N. Nagaosa, Symmetry and Topology in Superconductors—Odd-Frequency Pairing and Edge States—, *J. Phys. Soc. Jpn.* **81**, 011013 (2012).
- [20] H. H. Sun, K. W. Zhang, L. H. Hu, C. Li, G. Y. Wang, H. Y. Ma, Z. A. Xu, C. L. Gao, D. D. Guan, Y. Y. Li, C. H. Liu, D. Qian, Y. Zhou, L. Fu, S. C. Zhang, F. C. Zhang, and J. F. Jia, Majorana Zero Mode Detected with Spin Selective Andreev Reflection in the Vortex of a Topologi-

- cal Superconductor, Phys. Rev. Lett. **116**, 257003 (2016).
- [21] M. Hell, M. Leijnse, and K. Flensberg, Two-Dimensional Platform for Networks of Majorana Bound States, Phys. Rev. Lett. **118**, 107701 (2017).
- [22] F. Pientka, A. Keselman, E. Berg, A. Yacoby, A. Stern, and B. I. Halperin, Topological Superconductivity in a Planar Josephson Junction, Phys. Rev. X **7**, 021032 (2017).
- [23] A. Fornieri, A. M. Whiticar, F. Setiawan, E. P. Marín, C. C. D. Asbjörn, A. Keselman, S. Gronin, C. Thomas, T. Wang, R. Kallaher, G. C. Gardner, E. Berg, M. J. Manfra, A. Stern, C. M. Marcus, and F. Nichele, Evidence of topological superconductivity in planar Josephson junctions, Nature **569**, 89 (2019).
- [24] D. Takagi, S. Tamura, and Y. Tanaka, Odd-frequency pairing and proximity effect in Kitaev chain systems including a topological critical point, Phys. Rev. B **101**, 024509 (2020).
- [25] C. Nayak, S. H. Simon, A. Stern, M. Freedman, and S. D. Sarma, Non-Abelian anyons and topological quantum computation, Rev. Mod. Phys. **80**, 1083 (2008).
- [26] R. Aguado and L. P. Kouwenhoven, Majorana qubits for topological quantum computing, Phys. Today **73**, 44 (2020).
- [27] J. Alicea, New directions in the pursuit of Majorana fermions in solid state systems, Rep. Prog. Phys. **75**, 076501 (2012).
- [28] C. W. J. Beenakker, Search for Majorana Fermions in Superconductors, Ann. Rev. Condens. Matter Phys. **4**, 113 (2013).
- [29] S. R. Elliott, M. Franz, *Colloquium*: Majorana fermions in nuclear, particle, and solid-state physics, Rev. Mod. Phys. **87**, 137 (2015).
- [30] Y. Ando and L. Fu, Topological Crystalline Insulators and Topological Superconductors: From Concepts to Materials, Annu. Rev. Condens. Matter Phys. **6**, 361 (2015).
- [31] M. Sato and Y. Ando, Topological superconductors: a review, Rep. Prog. Phys. **80**, 076501 (2017).
- [32] A. Y. Kitaev, Unpaired Majorana fermions in quantum wires, Phys. Usp. **44**, 131 (2001).
- [33] P. W. Anderson, Absence of Diffusion in Certain Random Lattices, Phys. Rev. **109**, 1492 (1958).
- [34] P. W. Brouwer, A. Furusaki, I. A. Gruzberg, and C. Mudry, Localization and Delocalization in Dirty Superconducting Wires, Phys. Rev. Lett. **85**, 1064 (2000).
- [35] O. Motrunich, K. Damle, and D. A. Huse, Griffiths effects and quantum critical points in dirty superconductors without spin-rotation invariance: One-dimensional examples, Phys. Rev. B **63**, 224204 (2001).
- [36] I. A. Gruzberg, N. Read, and S. Vishveshwara, Localization in disordered superconducting wires with broken spin-rotation symmetry, Phys. Rev. B **71**, 245124 (2005).
- [37] P. W. Brouwer, M. Duckheim, A. Romita, and F. von Oppen, Probability Distribution of Majorana End-State Energies in Disordered Wires, Phys. Rev. Lett. **107**, 196804 (2011).
- [38] A. Lobos, R. Lutchyn, and S. Das Sarma, Interplay of Disorder and Interaction in Majorana Quantum Wires, Phys. Rev. Lett. **109**, 146403 (2012).
- [39] W. DeGottardi, D. Sen and S. Vishveshwara, Majorana Fermions in Superconducting 1D Systems Having Periodic, Quasiperiodic, and Disordered Potentials, Phys. Rev. Lett. **110**, 146404 (2013).
- [40] W. DeGottardi, M. Thakurathi, S. Vishveshwara and D. Sen, Majorana fermions in superconducting wires: Effects of long-range hopping, broken time-reversal symmetry, and potential landscapes, Phys. Rev. B **88**, 165111 (2013).
- [41] M. Yahyavi, B. Hetényi, and B. Tanatar, Generalized Aubry-André-Harper model with modulated hopping and  $p$ -wave pairing, Phys. Rev. B **100**, 064202 (2019).
- [42] X. Cai, L.-J. Lang, S. Chen, and Y. Wang, Topological Superconductor to Anderson Localization Transition in One-Dimensional Incommensurate Lattices, Phys. Rev. Lett. **110**, 176403 (2013).
- [43] Q.-B. Zeng, S. Shu, and R. Lü, Quench dynamics in the Aubry-André-Harper model with  $p$ -wave superconductivity, New. J. Phys. **20**, 053012 (2018).
- [44] X. Tong, Y. Meng, X. Jiang, L. Chao, G. D. de M. Neto, and G. Xianlong, Dynamics of a quantum phase transition in the Aubry-André-Harper model with  $p$ -wave superconductivity, Phys. Rev. B **103**, 104202 (2021).
- [45] J. Wang, X.-J. Liu, G. Xianlong and H. Hu, Phase diagram of a non-Abelian Aubry-André-Harper model with  $p$ -wave superfluidity, Phys. Rev. B **93**, 104504 (2016).
- [46] T. E. Lee, Anomalous Edge State in a Non-Hermitian Lattice, Phys. Rev. Lett. **116**, 133903 (2016).
- [47] S. Yao and Z. Wang, Edge States and Topological Invariants of Non-Hermitian Systems, Phys. Rev. Lett. **121**, 086803 (2018).
- [48] K. Yokomizo and S. Murakami, Non-Bloch Band Theory of Non-Hermitian Systems, Phys. Rev. Lett. **123**, 066404 (2019).
- [49] D. S. Borgnia, A. J. Kruchkov, and R.-J. Slager, Non-Hermitian Boundary Modes and Topology, Phys. Rev. Lett. **124**, 056802 (2020).
- [50] H. Menke and M. M. Hirschmann, Topological quantum wires with balanced gain and loss, Phys. Rev. B **95**, 174506 (2017).
- [51] T. Liu, S. Cheng, H. Guo, and G. Xianlong, Fate of Majorana zero modes, exact location of critical states, and unconventional real-complex transition in non-Hermitian quasiperiodic lattices, Phys. Rev. B **103**, 104203 (2021).
- [52] L.-J. Lang and S. Chen, Majorana fermions in density-modulated  $p$ -wave superconducting wires, Phys. Rev. B **126**, 205135 (2012).
- [53] S. Aubry and G. André, Analyticity breaking and Anderson localization in incommensurate lattices, Ann. Isr. Phys. Soc. **3**, 18 (1980).
- [54] C. Paige and C. V. Loan, A Schur decomposition for Hamiltonian matrices, Linear Algeb. and Its Appl. **41**, 11 (1981).
- [55] F. Alex An, K. Padavić, E. J. Meier, S. Hegde, S. Ganeshan, J. H. Pixley, S. Vishveshwara, and B. Gadway, Interactions and Mobility Edges: Observing the Generalized Aubry-André Model, Phys. Rev. Lett. **126**, 040603 (2021).